```
_{2}^{49}008). It has a limb darkened angular diameter of
   \pm 0.15^{2}
   _2009 which means that its ubtends the largest angular diameter of any star in the northern sky apart from the Sun. It is by far the account of the sun 
   formation region OriOB1 [?, see, e.g., ]] hoogerwer f_2000, and was a spectral type O9V star while on the main sequence, where i=20\ M_{\odot}
 18M_{\odot}
    2\times
 10^{-5} g_{\odot}
   \widetilde{\overset{\sim}{10}}{\overset{\sim}{10}} M_{\odot} yr^{-1}
   _{2}001.Likemostlate-
\begin{array}{c} \textbf{type} evolved stars, Betelgeuse's terminal wind velocity}_{vesc} \\ \textbf{2?} \\ \textbf{2} \\ \vdots \\ \textbf{2} \\ \vdots \\ \textbf{3} \\ \vdots \\ \textbf{4} \\ \vdots \\ \textbf{5} \end{array}
                                                                                                                                                                                                                                               ^^.?^.?.?^.?.?.?.?.?.?.?.?.
                                                                                                                   0.45 \pm 0.4
                                                                                                                                                       0/
                                                                                                                   \begin{array}{c} 5.07 \pm 1.1 \\ 197 \pm 45 \\ \sim 20 \end{array}
   \pi
   M_{\star}M_{\odot}
                                                                                                         \begin{array}{c} \sim 18 \\ 43.33 \pm 0.04 \end{array}
    M_{\star}M_{\odot}
   \theta_{UD}
 \overset{\theta LD}{R_{\star}R_{\odot}}
                                                                                                         44.28 \pm 0.15
   T_{eff}
   _{10}\, L_{\star}/L_{\odot}
                                                                                                            5.10 \pm 0.22
 v_{rad}^{-1}
                                                                                                                                                                                                                                               ?
                                                                                                                                                                                                                                               ?
                                                                                                                    20.7 \pm 0.4
v_{esc}
   T_{wind}^{-1}
                                                                                                                                 < 4000
 \dot{M}_{\star} \dot{M}_{\odot}^{-1}
H_{\star} R_{\star}
                                                                                                                       3\times 10^{-6}
                                                                                                                                                                                                                                               ?
                                                                                                              0.05 \pm 0.14
   B_{\star}
                                                                                              -3 \to +2 \pm 0.5
                                                                                                                                                  . . .
                                                                                                                                                  . . .
                                                                                                                   \begin{array}{c} 6 \pm 1 \\ 525 \pm 250 \\ 700 \pm 300 \end{array}
   1213
   1617
   1618
 \begin{array}{l} \widetilde{17} \\ 1998, which implies that it is probably experiencing very limited action of a solar-like dynamo. This rotation periodis in stark contrast to the equatorial solar rotation rate which is just 24.5 days. Its larger adius of the contrast of the equatorial solar rotation rate which is just 24.5 days. Its larger adius of the contrast rotation rate which is just 24.5 days. Its larger adius of the contrast rotation rate which is just 24.5 days. Its larger adius of the contrast rotation rate which is just 24.5 days. Its larger adius of the contrast rotation rate which is just 24.5 days. Its larger adius of the contrast rotation rate which is just 24.5 days. Its larger adius of the contrast rotation rate which is just 24.5 days. Its larger adius of the contrast rotation rate which is just 24.5 days. Its larger adius of the contrast rotation rate which is just 24.5 days. Its larger adius of the contrast rotation rate which is just 24.5 days. Its larger adius of the contrast rotation rate which is just 24.5 days. Its larger adius of the contrast rotation rate which is just 24.5 days. Its larger adius of the contrast rotation rate which is just 24.5 days. Its larger adius of the contrast rotation rate which is just 24.5 days. Its larger adius of the contrast rotation rate which is just 24.5 days. Its larger adius adjust 24.5 days. Its larger adjust 24.5 d
 H_{\star} \sim 0.01 R_{\star}
 \begin{array}{l} \vdots\\ 2007. \cite{1.5cm}\\ 2007. \cite{1.5cm}\\ 1007. \cite{1.5c
   70.8000 \atop 1982, hartmann_1984. In fact, high resolution UV photons cattering imaging with the HST partially resolved the hotch romosphere. The contraction of the c
 ^{1996.However}, \cite{Postation} \cite{Vphotonscatter} \cite{Vp
    2500
   \widetilde{5.4} \times 10^{-4}
```

 $\frac{1}{2}001$ , bowers  $\frac{1}{1}987$ , and low molecular abundances knapp  $\frac{1}{1}980$ , huggins  $\frac{1}{1}987$ , jewell  $\frac{1}{1}991$ , lambert  $\frac{1}{1}978$ . However, it is known to

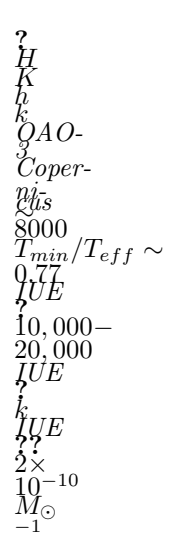
 $\begin{array}{c} \bar{0}.1R_{\star} \\ \bar{1}500 \\ \bar{1}.4R_{\star} \end{array}$ 

```
_2009. The data were compared to 3-Dhydrodynamical simulations by \cite{Concluded}, resulting in the detection of a granulation pattern on the surface. They concluded that the property of 
                                 5-
1.54-
2.17μm
R<sub>*</sub>
200 Th
                                      _2009. The septume shave been attributed to the action of giant convection cells. The rmal infrared VLT (\lambda =
                                 20\mu m
                                      100R_{\star}
                                      ^{2.0}_{2011}, while Herschelimages show a chaotic dust distribution far out in the circumstellar envelope, i.e., beyond_{\star}
                                   \frac{1}{2} \tilde{0} 12. A conclusion that can be drawn from the sest udies is the constant presence of inhomogenities in the circumstellar environment of the constant presence 
                                      _2006 is a millimeter interferometer located at Cedar Flatine astern California at an elevation of 2200\,m. The array consists of the contraction of the contraction
                                      115GHz(3mm)and215-
                                   270 GHz (1.3 mm). Eight additional 3.5 mantennask nown as the Sunyaev-Zel'dovich Array (SZA) can also be added to CARM A for continuum observations at 26-20 february (SZA) can also be added to CARM A for continuum observations at 26-20 february (SZA) can also be added to CARM A for continuum observations at 26-20 february (SZA) can also be added to CARM A for continuum observations at 26-20 february (SZA) can also be added to CARM A for continuum observations at 26-20 february (SZA) can also be added to CARM A for continuum observations at 26-20 february (SZA) can also be added to CARM A for continuum observations at 26-20 february (SZA) can also be added to CARM A for continuum observations at 26-20 february (SZA) can also be added to CARM A for continuum observations at 26-20 february (SZA) can also be added to CARM A for continuum observations at 26-20 february (SZA) can also be added to CARM A for continuum observations at 26-20 february (SZA) can also be added to CARM A february (SZA) can also be added to CARM A february (SZA) can also be added to CARM A february (SZA) can also be added to CARM A february (SZA) can also be added to CARM A february (SZA) can also be added to CARM A february (SZA) can also be added to CARM A february (SZA) can also be added to CARM A february (SZA) can also be added to CARM A february (SZA) can also be added to CARM A february (SZA) can also be added to CARM A february (SZA) can also be added to CARM A february (SZA) can also be added to CARM A february (SZA) can also be added to CARM A february (SZA) can also be added to CARM A february (SZA) can also be added to CARM A february (SZA) can also be added to CARM A february (SZA) can also be added to CARM A february (SZA) can also be added to CARM A february (SZA) can also be added to CARM A february (SZA) can also be added to CARM A february (SZA) can also be added to CARM A february (SZA) can also be added to CARM A february (SZA) can also be added to CARM A february (SZA) can also be added to CARM A february (SZA) can als
                                   115GHz(3mm). The different sizes of the CARMA antennas make sita heterogeneous array with a total collecting are a equivalent to the contract of the contrac
                                   element \`CAR\'MA array has 3 different primary beams), there are a number of a dvantages. Such an array samples shorter space of the such as a such a such a such as a such a such as a such a such as a such
                                      _{t}emplate/3/carma_{c}onfigs.ps[CARMA array configurations used] The three CARMA array configurations used to study to the configuration of the configura
                             \begin{array}{c} mid-\\ dle\\ B_{max}\\ 148\\ \end{array}
                                        right
                                      \frac{B_{min}}{370}
                                 template/3/carma_layout.ps[Layout of an tenna pads for CARMA] The layout of an tenna pads for CARMA and a visual of the street of the street
                                        (230 \, GHz/\nu)
                      \vec{B}_{max}
\vec{B}_{min}
                                   \dot{\theta}_{HPBW}
                                   \theta_{LAS}
                                      _{HPBW}^{50} \times (230\,GHz/
u) _{HPBW}^{10} _{HPBW}^{50} \times (230\,GHz/
u) _{HPBW}^{10} _{HPBW}^{10} _{HPBW}^{50} _{HPBW}^{50
                                   polarization SIS receivers for the 3 mm band. The tuning ranges of the 1\,mm and 3\,mm receivers are GHz and\,GHz, respectively the following the following ranges of the 1\,mm and 3\,mm receivers are GHz and\,GHz, respectively the following ranges of the 1\,mm and 3\,mm receivers are GHz and\,GHz, respectively the following ranges of the 1\,mm and 3\,mm receivers are GHz and\,GHz, respectively the following ranges of the 1\,mm and 3\,mm receivers are GHz and\,GHz, respectively the following ranges of the 1\,mm and 3\,mm receivers are GHz and GHz, respectively the following ranges of the 1\,mm and 3\,mm receivers are GHz and GHz, respectively the 1\,mm and 3\,mm receivers are GHz and GHz, respectively the 1\,mm and 3\,mm receivers are GHz and GHz, respectively the 1\,mm and 3\,mm receivers are GHz and GHz, respectively the 1\,mm and 3\,mm receivers are GHz and GHz, respectively the 1\,mm and 3\,mm receivers are GHz and GHz.
                                   \nu_{IF}^{RT} = \nu_{RF} \pm \nu_{LO1}.
(1)
                                      G_{RF}(\nu_{RF})

\begin{array}{l}
G_{IF} \nu_{IF} \\
\nu_{BB} = \nu_{IF} \pm \nu_{LO2}.
\end{array}

                                      _{2009.} The power measurement, sys _{1216}^{1216} J =
                                 2.1
4.4
0.9
                                   \tilde{\tilde{a}}^2
                                   <u>.</u>....
                                   1.3km\,s^{-1}
                               0.65km s^{-1}
0.65km s^{-1}
0.65km s^{-1}
                                      \widetilde{2.5}
                                              (970; baade_1996; eaton_2008; crowley_2008). Eventhough these systems of ferus the best opportunity to obtain in formation on the standard property of the standard prop
                                      \'1999. In order to avoid the assumed additional complexities of a companion, we have selected two single luminosity class III reconstructions and the companion of the compani
                                          Arcturus(\alpha
                                   Q.14
```

 $7R_{\star}$ 



 $_template/3/drake_mg.ps[IUEMgiikline and Drake models]IUEMgiikline profile for Arcturus over-plotted with the models of the profile for Arcturus over-plotted with the profil$ 

```
 \begin{array}{l} IUE \\ 6\times \\ 10^4 \\ 1\times \\ 10^5 \\ HST \\ 3\sigma \\ 2003. It appears that Arcturus has been able to sustain a modest level of magnetic activity. Three measurements for the mean lost <math>0.26, 0.43\pm \\ 0.16, \\ -0.23\pm \\ 0.20 \\ 2011, and a magnetic cycle with a period of \geq \\ 14 \\ 2008. \end{array}
```